

Quantum electrodynamics in a whispering gallery microcavity coated with a polymer nanolayer

Yun-Feng Xiao^{1,*}, Chang-Ling Zou², Peng Xue³, Lixin Xiao¹,
Yan Li¹, Chun-Hua Dong², Zheng-Fu Han², and Qihuang Gong^{1†}
¹*State Key Laboratory for Artificial Microstructure and Mesoscopic Physics,
School of Physics, Peking University, Beijing 100871, P. R. China.*

²*Key Lab of Quantum Information, CAS, University of Science and Technology of China, Hefei 230026, P. R. China. and*

³*Department of Physics, Southeast University, Nanjing 211189, P. R. China*

Quasi-TE and TM fundamental whispering gallery modes in a polymer coated silica microtoroid are theoretically investigated, and demonstrated to possess very high quality factors. The existence of nanometer thickness layer not only reduces the cavity mode volume evidently, but also draws the the maximal electric field's position of the mode to the outside of the silica toroid where single quantum dots or nanocrystals are located. Both effects result in a strongly enhanced coherent interaction between single dipole (for example, single defect center in diamond crystal) and the quantized cavity mode. Since the coated microtoroid is highly feasible and robust in experiment, it may offer an excellent platform to study strong-coupling cavity QED, quantum information and quantum computation.

PACS numbers: 03.67.Lx, 42.50.Pq, 42.60.Da, 42.55.Sa

I. INTRODUCTION

When single neutral atoms or quantum dots are strongly coupled to quantized electromagnetic fields through dipole-interaction inside a high- Q cavity, it has long been a central paradigm for the study of open quantum systems and plays a leading role in defining research goals. This coherent interaction is referred to cavity quantum electrodynamics (QED), which offers an almost ideal system for the generation of entangled states and implementation of small-scale quantum information processors recently [1, 2]. The reason is that atoms are particularly well suited for storing qubits in long-lived internal states, and photons are the best qubit carrier for fast and reliable communication over long distances.

For cavity QED study, three representative optical microcavities have been proposed and investigated up to the present [3]: the conventional Fabre-Perot (FP)-type cavities consisting of two concave dielectric mirrors at a distance of tens of microns, the nanoscale optical cavities in photonic crystal where a dot or line defect is introduced, and the dielectric optical microcavities supporting whispering gallery modes (WGMs). Over past few years, the strong coupling regime (i.e., the light-matter coherent interaction strength exceeds both the cavity and dipole decay rates) has been realized using either FP-type microcavities [4–7] or photonic crystal nanocavities [8–10]. Experiments with single atoms have been at the forefront of these advances with the use of optical FP resonators. Nevertheless, the extremely technical challenges will be typically involved in further improving the resonators and scaling to large numbers of microcavi-

ties. Thus there is an increasing interest in the development of alternative microcavity systems. WGMs in a rotational-symmetry geometry exhibit exciting characteristic such as extremely high quality factor, small mode volume, and excellent scalability [11, 12]. As a result, this system has been of particular interest to reach the strong light-matter coherent interaction. In experiment, single cold caesiums coupled to a silica microtoroid [13], nanocrystalline quantum dots coupled to microsphere cavities [14, 15], and single quantum dots coupled microdisks [16, 17] have been reported.

Except single etched quantum dots embedding in the microdisks, single cold atoms or nanocrystalline quantum dots are locating on the outer surface of cavity. In this case, only weak evanescent field of the cavity mode is used to interact with atoms/quantum dots, and thus the coherent coupling strength can not reach its maximum. In this paper, we study cavity QED in a silica toroid microcavity coated with a high-refractive-index nanolayer. The idea is at least twofold. First, with an increasing in nanolayer thickness, the optical field of a WGM in the coated microtoroid moves to outside the silica surface where quantum dots are located, which results in strongly enhancing the coherent interaction strength between the WGM and coupled quantum dots. Second, the high-refractive-index layer compresses the radial optical field of the WGM, which may reduce the mode volume.

II. MODES IN A NANOLAYER-COATED MICROTOROID

The geometry of the proposed nanolayer-coated microcavity is shown in Fig. 1. A silica microtoroid with a refraction index n_1 can be prepared on a silicon chip through the standard photolithography technique and CO₂ laser reflow [18], with the major radius R and the

*Electronic address: yfxiao@pku.edu.cn

†Electronic address: qhgong@pku.edu.cn

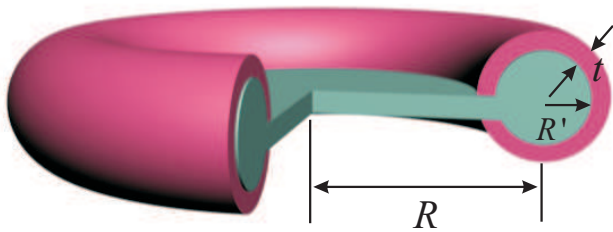


FIG. 1: (Color online) Schematic illustration of a polymer coated silica toroidal microcavity. The major and minor radii of silica toroid are R and R' , respectively. The coating thickness is t . The refractive indexes of silica, polymer and air are $n_1 = 1.4564$, $n_2 = 1.59$, and $n_3 = 1$, respectively.

minor radius R' . The toroidal microcavity is then coated by a layer of polymer material, such as SU-8, which is transparent over visible to infrared [19], and has a large refraction index n_2 . The coating thickness is a nanometer scaling, denoted by t . Beyond the coated polymer, it is the air with refraction index n_3 . Recently, this type of polymer coated microcavities has been utilized for enhancing the sensitivity of a cavity-based biosensor [20], suppressing the thermal-optic noise in silica resonator [21], and observing electromagnetically induced transparency-like effect in a single cavity [22]. In this paper, however, we focus on the cavity QED with coated microcavity. In the following study, we vary the major radius R and the coating thickness t , but fix the size of minor radius R' for simplicity.

In order to investigate the properties of coated microtoroids for cavity QED, we focus our attention on the dipole transition with a zero-phonon line at 637 nm of the nitrogen-vacancy (NV) defect in diamond nanocrystal. NV centers are well suited for cavity QED and quantum information because they have a long-lived spin triplet (over 0.35 ms) in its electronic ground state [23, 24] that can be initialized, manipulated, and read out through highly stable optical and microwave excitations at room temperature. Experimentally, single NV centers have been studied as a photostable single-photon source without photobleaching for quantum communication [25, 26], quantum register, Rabi oscillations and conditional two-qubit quantum gates for quantum information and computation [27–31]. Single NV center strongly coupling to a cavity mode has also been demonstrated [15, 32, 33]. In essence, the investigation of the coupling between a NV center and a cavity mode field can be specified by three cavity-QED parameters: the quality factors Q of the cavity mode, the mode volume V_m , and the effective dipole-cavity coupling coefficient $g(\vec{r})$ at the NV center's location \vec{r} . In whispering gallery cavity QED experiment, the NV centers typically interact only with the evanescent field of the cavity mode. Thus, we assume that single NV centers are located near the microcavity surface.

Different from a spherical microcavity, there is no analytic solution for a microtoroid though the perturbative analytic theory has been proposed [34]. For a

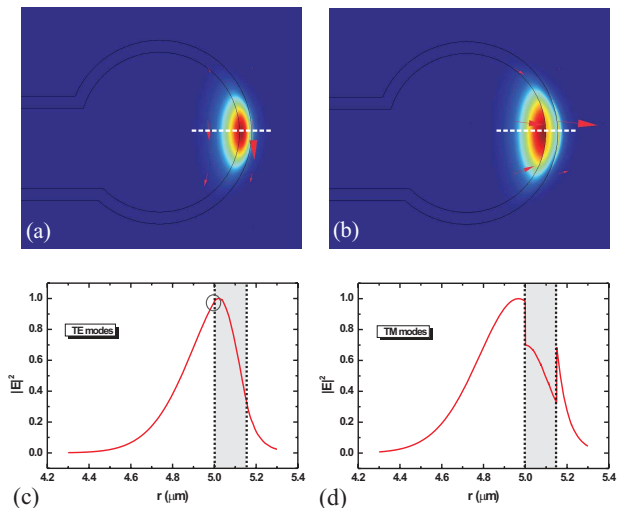


FIG. 2: (Color online) (a)-(b): False-color representations of the normalized squared transverse electric fields for quasi-TE and TM modes, respectively, where the arrows show the directions of the electric fields. (c)-(d): The distributions of the normalized squared electric fields along the radial direction (dashed lines in (a) and (b)) for quasi-TE and TM modes, respectively. The dotted lines denote the boundary positions. Here $R = 4 \mu\text{m}$, $R' = 1 \mu\text{m}$, and $t = 150 \text{ nm}$.

nanolayer coated microtoroid, the perturbative analytic theory may still work but it should be much more complicated. Therefore, to explicitly achieve the useful metrics of the coated toroidal microcavity, such as resonant wavelengths, quality factors and mode volumes, we resort to numerical simulations. In Figs. 2a and 2b, by using a full-vectorial finite element method (FEM), we show two typical WGMs in a coated silica microtoroid in the wavelength of 637 nm. Here the major and minor radii of the silica toroid are set as 4 and 1 μm , respectively, and the coating thickness is 150 nm. Similar to an uncoated microtoroid, the mode field in the coated toroidal microcavity can be treated as quasi-TE or quasi-TM modes. For quasi-TE modes, the dominant electric field components are in the azimuthal vertical direction, as shown by the red arrows in Fig. 2a; while for quasi-TM modes, the dominant electric fields are in the radial direction, as shown in Fig. 2b. Their normalized squared transverse electric fields are also plotted in Figs. 2c and 2d, respectively. It can be found two important indications. On one hand, for quasi-TE modes, the electric field shows a relatively smooth boundary change along the radial direction since it dominates in the azimuthal vertical (transverse) direction which has continuous nature of dielectric boundary $E_{i,\text{tran}} = E_{j,\text{tran}}$. Nevertheless, there is some minor discontinuity at the boundary interface, as indicated in the ellipse in Fig. 2c. The reason is that the toroidal geometry has been strongly compressed with respect to a microsphere, and strictly speaking, the quasi-TE modes are hybrid modes. As a result, the non-transverse electric field does exist though they remain rel-

atively small. For quasi-TM modes, as expected, a large discontinuity of the electric fields on the boundary occurs. This is because the dominant electric field component of the quasi-TM mode is in the radial direction (normal to the boundary interface) which satisfies the discontinuous boundary condition $n_i^2 E_{i,\text{normal}} = n_j^2 E_{j,\text{normal}}$. On the other hand, in the presence of the nanolayer coating, the maximum of the electric field of the WGMs further move to the silica-polymer boundary interface compared to that of an uncoated silica toroidal microcavity. For quasi-TE modes, the maximum can even be located in the polymer layer for a smaller coating thickness. This qualitatively demonstrates the first motivation of this paper that the effective dipole-cavity coupling rate when the NV center is placed the outer surface of the silica can be increased for a coated microcavity. In the following sections, we in turn discuss the quality factors Q and the mode volume V_m of the WGMs in the coated silica microtoroid, and the effective dipole-cavity coupling rate $g(\vec{r} = R + R')$. Also, we will only consider the fundamental modes for both the quasi-polarizations, as they possess the smallest mode volumes and thus the largest coupling strengths.

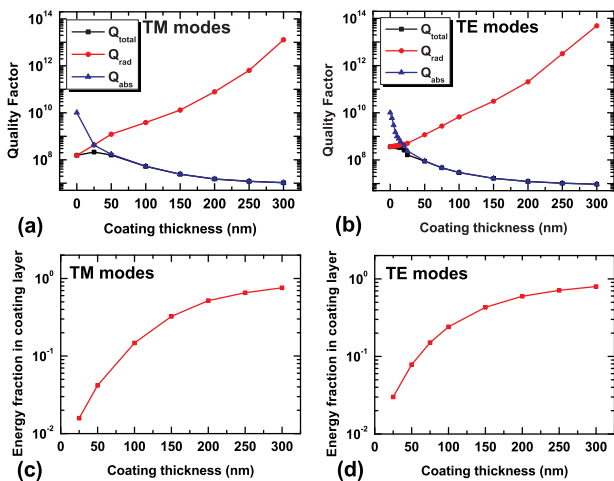


FIG. 3: (Color online) (a)-(b): Quality factors for the fundamental quasi-TM/TE WGMs in polymer coated silica microtoroids when the coating thickness t is changed. The square, circle and triangle represent the total, radiation, and absorption related quality factors, respectively. (c)-(d): The energy fractions in the coating polymer depending on the coating thickness for TM and TE modes, respectively. Here $R = 4 \mu\text{m}$ and $R' = 1 \mu\text{m}$.

III. QUALITY FACTORS OF THE MODES

For cavity QED experiment, the quality factor of the WGM is one of important parameters. It is related to the several different optical loss mechanisms. In general, the overall quality factor can be calculated by adding the

different contributions in the following express

$$\frac{1}{Q_{\text{total}}} = \frac{1}{Q_{\text{rad}}} + \frac{1}{Q_{\text{mat}}}, \quad (1)$$

and

$$\frac{1}{Q_{\text{mat}}} = \frac{1}{Q_{\text{s.s}}} + \frac{1}{Q_{\text{w}}} + \frac{1}{Q_{\text{abs}}}, \quad (2)$$

where Q_{rad} is due to purely radiative losses for an ideal dielectric microcavity; Q_{mat} results from non-ideal material properties, including the contributions the scattering losses from residual surface inhomogeneities ($Q_{\text{s.s}}$), absorption losses due to water on the outer surface of the coating polymer (Q_{w}), and bulk absorption in the silica and polymer material (Q_{abs}). Typically, the silica toroid has an atom-scale surface due to its laser-reflow fabrication, and this smooth surface will transfer to the polymer, resulting a very small scattering losses from residual surface inhomogeneities; on the other hand, the water absorption can be suppressed in a vacuum environment. Thus here we consider only radiation-related quality factor Q_{rad} , material absorption-related quality factor Q_{abs} , and the total quality factor Q_{total} . Since in this paper we focus on the dipole transition of NV defect at center wavelength 637 nm, we set the absorption losses of silica and SU-8 10^{-5} and 0.01 dB/cm, respectively.

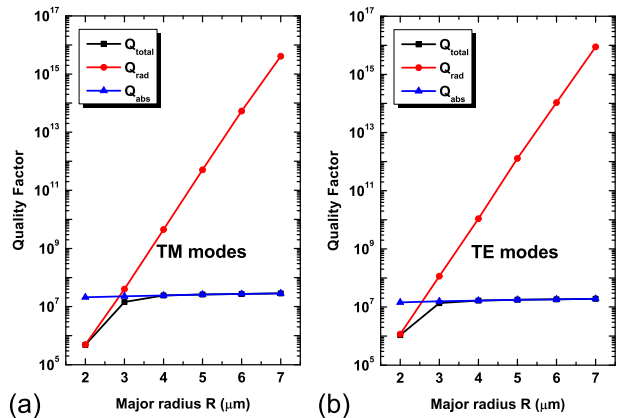


FIG. 4: (Color online) (a)-(b): Quality factors for the fundamental quasi-TM/TE WGMs in polymer coated silica microtoroids when the major radius R is changed. The square, circle and triangle represent the total, radiation, and absorption related quality factors, respectively. (c)-(d): The energy fractions in the coating polymer depending on the coating thickness for TM and TE modes, respectively. Here $t = 150 \text{ nm}$ and $R' = 1 \mu\text{m}$.

In order to study how the quality factors depend on the coating thickness t , Figs. 3a and 3b illustrate Q_{total} , Q_{rad} , and Q_{abs} for quasi-TM and TE modes, respectively. For an uncoated silica toroid ($t = 0 \text{ nm}$), the total quality factor Q_{total} behaves the radiation loss limited (i.e., $Q_{\text{total}} \sim Q_{\text{rad}}$) since the absorption of silica is much smaller (resulting $Q_{\text{abs}} > 10^{10}$) for both the TM and TE

modes. This is valid if we neglect the surface scattering loss for a small sized microsphere. For the coated silica toroid with a large coating thickness, for example $t > 50$ nm, however, Q_{total} is limited by the absorption loss (thus $Q_{\text{total}} \sim Q_{\text{abs}}$) since in this case the absorption of polymer plays the dominant role in the whole loss mechanisms. This can be partly demonstrated in Figs. 3c and 3d. With increasing the coating thickness, more and more energy distributes in the nanolayer. When the thickness t ranges from 0 and 50 nm, it is a little complicated. There is a tradeoff between Q_{rad} and Q_{abs} . In general, with increasing the thickness t , the radiation loss rapidly decreases due to the protection of the high-index nanolayer (leading to a quick increasing of Q_{rad}), while the absorption loss increases because more mode energy distributes in the relatively high loss polymer layer (resulting in a decreasing of Q_{abs}). For both the modes, when the coating thickness t increases from 0, the total quality factor Q_{total} first shows a slight increase, because the increasing rate of the absorption loss is less than the decreasing rate of the radiation loss. At a certain thickness t (~ 25 and 5 nm for quasi-TM and TE modes, respectively), Q_{total} reaches the maximum when the increasing rate of the absorption loss is right compensated by the decreasing rate of the radiation loss. Then with the coating thickness increases further, Q_{total} decreases because the increasing rate of the absorption loss exceeds the decreasing rate of the radiation loss.

Quality factors are also dependent on the the size of toroid. Here we give the coating thickness $t = 150$ nm and the minor radius $R' = 1 \mu\text{m}$, and study their dependence on the major radius R , as shown in Figs. 4a and 4b, for quasi-TM and TE modes, respectively. We have the following results. First, the absorption related quality Q_{abs} only experiences slight increase with the major radius R changing. Second, at small major radius, the radiation loss is much higher than the absorption loss, resulting in the radiation-limited total quality factor Q_{total} ($Q_{\text{total}} \sim Q_{\text{rad}}$). Third, when the major radius R increases, the radiation loss decreases and becomes comparable with the absorption loss. In this case, Q_{total} increases fast with increasing R . Finally, when R is large enough, the radiation loss becomes much lower than the absorption loss, resulting in the absorption-limited Q_{total} ($Q_{\text{total}} \sim Q_{\text{abs}}$).

IV. MODAL VOLUMES OF THE MODES

The other important parameter for cavity QED is the modal volume V_{m} of WGM, defined as

$$V_{\text{m}} \equiv \frac{\int_V |n(\vec{r})E(\vec{r})|^2 dV}{|n(\vec{r})E(\vec{r})|_{\text{max}}^2}. \quad (3)$$

Using Eq. (3), the modal volume is numerically calculated in Fig. 5 for different coating thickness and major radius. The mode volume may increase or decrease at

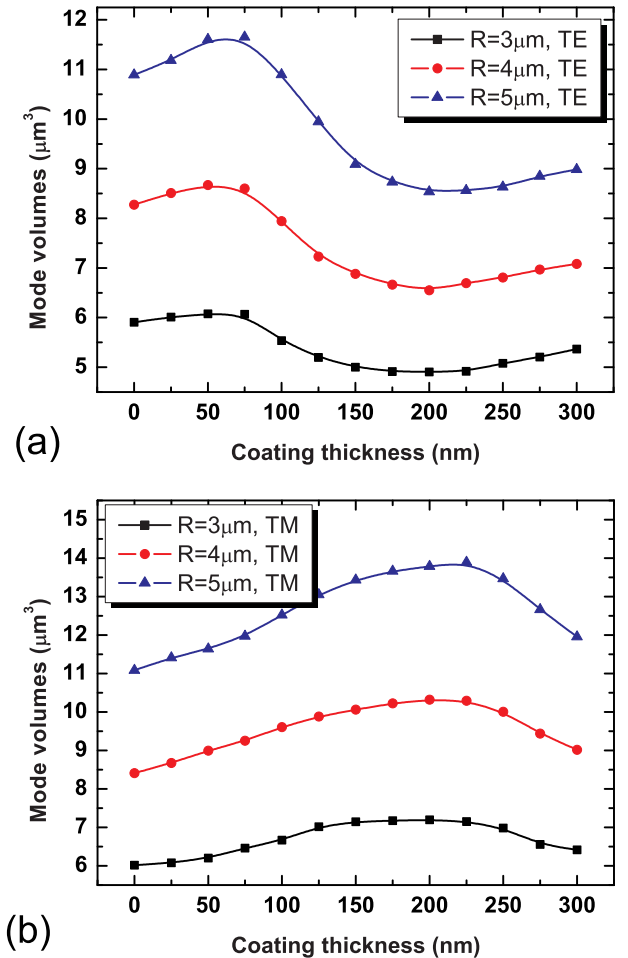


FIG. 5: (Color online) (a)-(b): The mode volumes for quasi-TE and TM modes, respectively. Here $R' = 1 \mu\text{m}$.

different coating thickness. To better explain this phenomenon, we note that the mode volume also could be approximately expressed as $2\pi R_{\text{eff}} A_{\text{eff}}$, where R_{eff} is the effective radius of the ring-type cavity, and A_{eff} represents the effective mode area in the cross section (see Figs. 1a and 1b showing the cross sectional distributions for quasi-TE and TM mode fields). Typically, there are the following three regions. (i) When the SU-8 polymer coating thickness on the silica microtoroid is small, the mode volume first exhibits an obvious increasing with t for both the quasi-TE and TM modes. This is due to the increase of the effective radius R_{eff} , approximately proportional to $R + R' + t$, while A_{eff} keeps almost unchanged (minor energy in the coating nanolayer). (ii) With the coating thickness increasing, it is interesting that V_{m} starts to decrease. This can be understood by considering the fact that the refractive index n_2 of SU-8 polymer is larger than the silica. The coating polymer film forms a kind of film waveguide, where light could be well confined in the film by the total internal reflection at both the polymer-silica and polymer-silica interfaces. The guiding modes in film must satisfy the cut-off con-

ditions. As a result, when t is as large as 200 nm, the most field energy of the mode could be well confined in the film, resulting in the reduced mode area A_{eff} . The decreasing rate of A_{eff} exceeds the increasing rate of R_{eff} , so that the mode volume decreases in a range of t . (iii) Finally, with t keeping increased, the polymer-silica interface plays a minor role in confining light, so the mode volume increases again with t (The decreasing rate of A_{eff} is less the increasing rate of R_{eff} again). The change of the mode volumes for quasi-TE and TM polarized modes are slightly different, originating from the different cut-off condition of guide mode for different polarization.

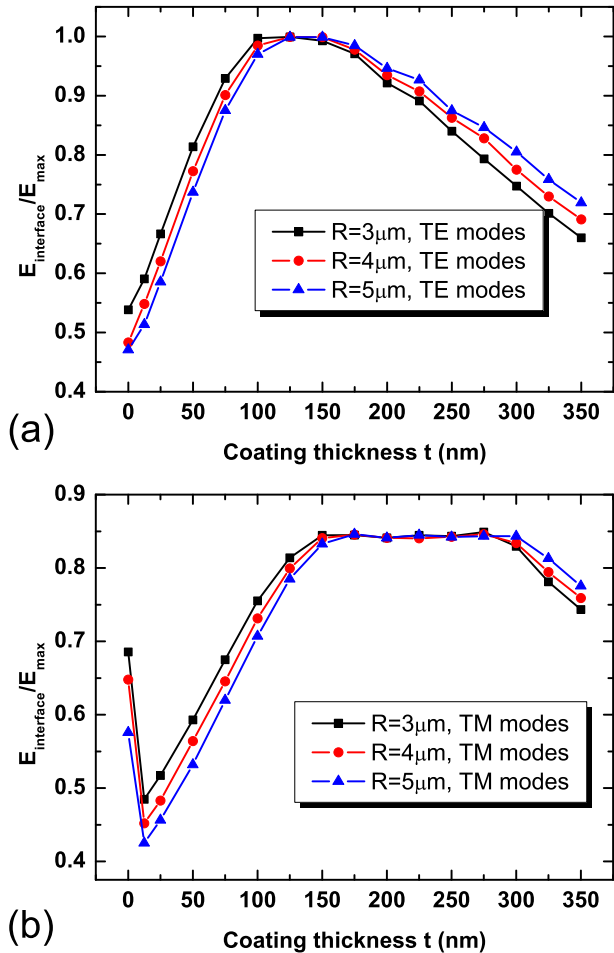


FIG. 6: (Color online) (a)-(b): Electric field at silica-polymer outer interface normalized to the maximum for quasi-TE and TM modes, respectively. Here $R' = 1 \mu\text{m}$.

V. SINGLE-PHOTON COHERENT COUPLING STRENGTH AND THE STRONG-COUPLING REGIME

As we mentioned above, the ultimate goal of this paper is to employ the WGMs of coated silica microtoroids as cavity modes for achieving strong coupling to NV centers

within the setting of cavity QED. Based on the above basic results, we can analyze the coupling coefficient $g(\vec{r})$, which is the coupling frequency of a NV center to a particular cavity mode and corresponds to one-half the single-photon Rabi frequency. Since we assume that the NV center in a diamond nanocrystal is located just at the outer surface of the silica toroid and interacts with a WGM, we can define an effective coupling coefficient g_{eff} , given by

$$g_{\text{eff}} = f \times g_{\text{max}}, \quad (4)$$

where the coefficient $f \equiv |E(\vec{r} = R + R')/E_{\text{max}}|$ defining the electric field at the outer silica-polymer interface normalized to the maximum, and $g_{\text{max}} \equiv (\mu^2 \omega_c / 2\hbar \epsilon V_m)^{1/2}$ with $\mu = 2.74 \times 10^{-29} \text{ C} \cdot \text{m}$ representing the dipole moment of NV center transition. In this section, we analyze f and g_{eff} depending on the coating thickness, and point out the potential of enhanced interaction between the NV center and the cavity mode in coated microcavity.

Figure 6 depicts the coefficient f when the major radius R is 3, 4, and 5 μm , and the coating thickness t ranges from 0 to 350 nm. For the quasi-TE mode, f first increases and then decreases smoothly. The underlying physics is that the maximal electric field's position of the quasi-TE mode is drawn to the outside from inside of the silica toroid when the coating thickness is increasing. At a critical thickness (for instance, about 140 nm for $R = 4 \mu\text{m}$; this critical thickness slightly decreases for a smaller major radius), f approaches 1. In other words, the maximal electric field of the quasi-TE mode in this case locates at the silica-polymer interface. For the quasi-TM mode, it is a somewhat complicated. The coefficient f suddenly decreases in the presence of the nanometer-sized polymer coating layer, because of the discontinuous boundary condition for quasi-TM modes. Then f gradually increases and decreases similar to the quasi-TE mode, with increasing the coating thickness. Unlike the quasi-TE mode case, the maximal f is about 0.84, smaller than both n_1/n_2 and 1. The former is due to the presence of the non-radial electric field; while the latter is because of the discontinuous condition at silica-polymer boundary for the quasi-TM mode. Moreover, the electric field approaches the maximum within a very large range of the thickness t because the maximal electric field is exactly on the inner surface of the silica in this range.

By now, we have obtained the mode volume V_m and the coefficient f . Thus, we calculate the effective coupling coefficient g_{eff} according to Eq. (4), as shown in Fig. 7 for both the quasi-TE and TM modes. Since the coating nanolayer moves the maximum of the mode field to the silica-polymer interface, the effective coupling coefficient g_{eff} is greatly enhanced. For example, $g_{\text{eff}}/2\pi$ is of the order of GHz, and exceeds twice of the uncoated case for the quasi-TE mode. Thus, an enhanced interaction can be achieved between the WGM in the polymer-coated silica microtoroid and the coupled NV center.

We now turn to compare the effective coupling coefficient g_{eff} , the cavity mode decay rate $\kappa = \omega_c/Q$, and the

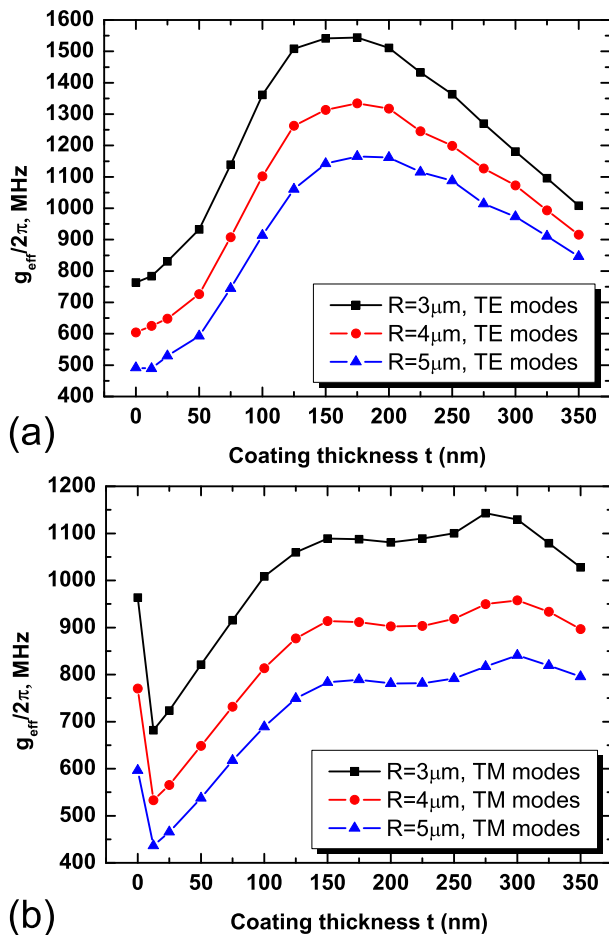


FIG. 7: (Color online) (a)-(b): Effective coupling coefficient g_{eff} when a single NV center locates at silica-polymer outer interface for quasi-TE and TM modes, respectively. Here $R' = 1 \mu\text{m}$.

transverse spontaneous emission rate $\gamma/2\pi = 13 \text{ MHz}$ for the dipole transition of NV center. For an intuitive comparison, we give an example showing quantitative values of them. For a polymer coated silica toroid with the parameters $R = 4 \mu\text{m}$, $R' = 1 \mu\text{m}$, $n_1 = 1.4564$, $n_2 = 1.59$, $n_3 = 1$, and the coating thickness $t = 100 \text{ nm}$, the effective coupling coefficient $g_{\text{eff,TE}}/2\pi \sim 1.1 \text{ GHz}$, the cavity decay rate $\kappa_{\text{TE}}/2\pi \sim 16 \text{ MHz}$ for a quasi-TE mode. Therefore, we can easily know that the coated silica toroid provides a good platform to achieve strong coupling regime because of $g_{\text{eff}} \gg \kappa, \gamma$.

VI. DISCUSSIONS AND EXPERIMENTAL FEASIBILITY

In the section above, we have theoretically demonstrated the enhanced NV center-WGM interaction for a coated silica microcavity. One may argue that the coating layer may also reduce the total quality factor Q_{total} of the cavity mode (as shown in Fig. 3), as well as an actu-

ally degraded g_{eff}/κ though g_{eff} can be improved. Thus more discussions on the coated microcavity are necessary. First, as pointed out in the section III, the total quality factor Q_{total} is limited by the SU-8 polymer absorption loss when the coating layer exceeds a certain thickness. As a result, Q_{total} has already reduced before the coupling system reaches the maximal coherent interaction (i.e., $f = f_{\text{max}}$). To exploit the enhanced-interaction advantages of the coated microcavity, SU-8 polymer coating is particularly suitable for a smaller silica toroid. For example, when the major radius $R = 2 \mu\text{m}$, $Q_{\text{total,TE}} \sim 10^6$ is still limited by the radiation losses even in the presence of the coating layer ($t = 150 \text{ nm}$). In this case, g_{eff} is strongly enhanced while κ keeps unchanged. Second, the reduction of κ can be relaxed by choosing a lower loss polymer, such as PMMA, leading to an almost unaffected Q_{total} (high up to 10^8) in a PMMA-coated silica microsphere [35]. Moreover, the refractive index of PMMA n_{PMMA} is about 1.49, which is closed to that of silica. Thus, not only the coefficient f_{TE} of the quasi-TE mode is increasing, but also f_{TE} can be further improved to $n_1/n_{\text{PMMA}} = 0.97$. Third, in an actual WGM cavity QED experiment, the deposition of quantum dots or diamond nanocrystals on the silica surface will inevitably degrade the total quality factor due to additional scattering losses, particularly for the case when silica cavity is immersed in a solution and then withdrawn [15, 36]. The existence of the polymer coating nanolayer, however, could recover the high total quality factor because the polymer nanolayer has a much more smooth surface which strongly reduce the scattering losses. Finally, compared to the conventional case that single atoms or nanocrystals are just adsorbed on the silica surface, the polymer nanolayer provides a protection, and single nanocrystals can stably locate on the silica surface.

It is also noted that the spontaneous emission rate given above is the value in the vacuum. When NV centers are placed in a dielectric, this rate will be changed, and can be approximately calculated as $\gamma = 9\varepsilon^{5/2}/(2\varepsilon + \varepsilon_{\text{NV}})^2\gamma_{\text{vac}}$ where ε and ε_{NV} are dielectric constants for surrounding medium and diamond [37], respectively. In the present paper, it is much more complex since the surrounding medium includes both silica and SU-8 polymer. Nevertheless, the difference is estimated about 50% if we take the average value for silica and SU-8 polymer. This change may partly reduce the cavity QED parameter $g_{\text{eff}}/\kappa\gamma$. The experimental realization of the polymer coating on the silica surface is the essential requirement in this study. Fortunately, polymer generally has a low surface tension enabling it to wet many materials including silica. Polymer-coated silica microcavities have been experimentally demonstrated recently [20, 21], and atomic force microscope scans reveal that the rms roughness of the polymer surface is comparable to that of bare silica. This makes our design has a highly experimental feasibility.

VII. SUMMARY

We have theoretically studied both the quasi-TE and TM fundamental whispering gallery modes in polymer coated silica microtoroids. Both the modes show very high quality factors and small mode volumes. It is of importance that the coated silica microcavity strongly enhances the coherent interaction strength at least twice between the WGM and the coupled NV center, compared to the uncoated microcavity, because (1) the coating layer (though nanometer sized) can draw the maximal electric field of the mode to the outside of the silica toroid where NV centers are located; (2) the mode volume can be reduced due to the high refraction index polymer layer. Furthermore, the coating nanolayer makes the cavity QED system more robust. Thus, the polymer coated microtoroid is highly feasible in experiment and offers a good platform to study strong-coupling cavity QED, quantum information and quantum computation.

Acknowledgments

The authors acknowledge financial support from the National Natural Science Foundation of China under Grant No. 10821062, the National Basic Research Program of China under Grant Nos. 2006CB921601, 2007CB307001 and 2009CB930504. Yun-Feng Xiao was also supported by the Research Fund for the Doctoral Program of Higher Education (No.20090001120004) and the Scientific Research Foundation for the Returned Overseas Chinese Scholars. Chang-Ling Zou, Chun-Hua Dong and Zheng-Fu Han were supported by the National fundamental Research Program of China under Grant No 2006CB921900; National Science Foundation of China under Grant No. 60537020 and 60621064. Peng Xue was also supported by National Natural Science Foundation of China under Grant No. 10944005.

-
- [1] J. M. Raimond, M. Brune, and S. Haroche, *Rev. Mod. Phys.* **73**, 565 (2001).
 - [2] H. Mabuchi and A. C. Doherty, *Science* **298**, 1372 (2002).
 - [3] K. J. Vahala, *Nature* **424**, 839 (2003).
 - [4] R. J. Thompson, G. Rempe, and H. J. Kimble, *Phys. Rev. Lett.* **68**, 1132 (1992).
 - [5] A. Boca, R. Miller, K. M. Birnbaum, A. D. Boozer, J. McKeever, and H. J. Kimble, *Phys. Rev. Lett.* **93**, 233603 (2004).
 - [6] J. P. Reithmaier *et al.*, *Nature* **432**, 197 (2004).
 - [7] P. Maunz, T. Puppe, I. Schuster, N. Syassen, P.W. H. Pinkse, and G. Rempe, *Phys. Rev. Lett.* **94**, 033002 (2005).
 - [8] T. Yoshie *et al.*, *Nature* **432**, 200 (2004).
 - [9] K. Hennessy *et al.*, *Nature* **445**, 896 (2007).
 - [10] A. Badolato *et al.*, *Science* **308**, 1158 (2005).
 - [11] J. R. Buck and H. J. Kimble, *Phys. Rev. A* **67**, 033806 (2003).
 - [12] S. M. Spillane *et al.*, *Phys. Rev. A* **71**, 013817 (2005).
 - [13] T. Aoki *et al.*, *Nature* **443**, 671 (2006).
 - [14] N. Le Thomas, U. Woggon, O. Schops, M. Artemyev, M. Kazes, and U. Banin, *Nano Lett.* **6**, 557 (2006).
 - [15] Y.-S. Park, A. K. Cook, and H. Wang, *Nano Lett.* **6**, 2075 (2006).
 - [16] E. Peter *et al.*, *Phys. Rev. Lett.* **95**, 067401 (2005).
 - [17] K. Srinivasan, and O. Painter, *Nature*. **450**, 862 (2007).
 - [18] D. K. Armani, T. J. Kippenberg, S. M. Spillane, and K. J. Vahala, *Nature*. **421**, 925 (2003).
 - [19] Om P. Parida and N. Bhat, International Conference on Optics and Photonics, CSIO, Chandigarh, India, 2009.
 - [20] O. Gaathon, J. Culic-Viskota, M. Mihnev, I. Teraoka, and S. Arnold, *Appl. Phys. Lett.* **89**, 223901 (2006).
 - [21] L. He, Y.-F. Xiao, C. Dong, J. Zhu, V. Gaddam, and L. Yang, *Appl. Phys. Lett.* **93**, 201102 (2008).
 - [22] Y.-F. Xiao, L. He, J. Zhu, and L. Yang, *Appl. Phys. Lett.* **94**, 231115 (2009)
 - [23] T. A. Kennedy, J. S. Colton, J. E. Butler, R. C. Linares and P. J. Doering, *Appl. Phys. Lett.* **83**, 4190 (2003).
 - [24] T. Gaebel *et al.*, *Nature Physics* **2**, 408 (2006).
 - [25] C. Kurtsiefer, S. Mayer, P. Zarda, and H. Weinfurter, *Phys. Rev. Lett.* **85**, 290 (2000).
 - [26] R. Brouri, A. Beveratos, J.-P. Poizat, and P. Grangier, *Opt. Lett.* **25**, 1294 (2000).
 - [27] F. Jelezko *et al.*, *Phys. Rev. Lett.* **93**, 130501 (2004).
 - [28] T. Gaebel *et al.*, *Nature Phys.* **2**, 408 (2006).
 - [29] R. Hanson, F. M. Mendoza, R. J. Epstein, D. D. Awschalom, *Phys. Rev. Lett.* **97**, 087601 (2006).
 - [30] R. J. Epstein, F. M. Mendoza, Y. K. Kato, D. D. Awschalom, *Nat. Phys.* **1**, 94 (2005).
 - [31] M. V. Gurudev Dutt *et al.*, *Science* **316**, 1312 (2007).
 - [32] P. E. Barclay, K.-M. C. Fu, C. Santori and R. G. Beausoleil, *Appl. Phys. Lett.* **95**, 191115 (2009).
 - [33] S. Schietinger, T. Schroder, and O. Benson, *Nano Lett.* **8**, 3911 (2008).
 - [34] B. Min, L. Yang, and K. Vahala, *Phys. Rev. A* **76**, 013823 (2007).
 - [35] C.-H. Dong *et al.*, submitted to *Appl. Phys. Lett.*
 - [36] B. Min *et al.*, *Appl. Phys. Lett.* **89**, 191124 (2006).
 - [37] A. Thranhardt, C. Ell, G. Khitrova, and H. M. Gibbs, *Phys. Rev. B* **65**, 035327 (2002).